

Electronic, Spectral and Structural Characteristics of Carbon Nanotubes: Gallium nitride as an optoelectronic Applications

Mohammed Jawad H. Kadhim

Department of Polymer and Petrochemical Industries, College of Materials Engineering, University of Babylon, Babil, Iraq.
alialahphy@yahoo.com

Ali S. Hasan

Department of Polymer and Petrochemical Industries, College of Materials Engineering, University of Babylon, Babil, Iraq.
alialahphy@yahoo.com

Q. A. AL-Jarwany

Department of Polymer and Petrochemical Industries, College of Materials Engineering, University of Babylon, Babil, Iraq.
mat.ali.salah@uobabylon.edu.iq

ABSTRACT

In this paper, the electronic, structural and spectral characteristics of GaN -grafted CNT prepared by chemical vapor deposition method, are studied. New models of CNT and CNT/GaN have been prepared and designed by DFT/B3LYP technique with SDD base groups. Surface morphology, electronic transitions, and structural characteristics have been determined by Gaussian 09 program package.

The electronic results gave the total energy, the energy gap, the highest occupied energy level (HOMO) and the lowest free energy level (LUMO). The surface morphology of thin CNT/GaN were observed by Scanning Electron Microscope (SEM), Furthermore, it has been utilized orbital analysis, counting the states density (DOS) to find the possible orbital hybridization for molecules, thus determining the optoelectronic effectiveness of the molecules under study. Through research, we can benefit from the results within optical applications and Nano film technology, with its high electronic and spectral characteristics.

Keywords:

Structural, electronic transitions properties; DFT; optoelectronic Applications

1-Introduction

The electrical structure of sp² hybridization carbon nanomaterials is highly delocalized, implying that they might be used as high mobility electronic materials. The capacity to adjust the band gap of semiconducting CNTs is also a plus. The wide variety of electronic characteristics of CNTs as just a function on the chiral vector, along with their quasi-one-dimensional structure, opens up a lot of possibilities for electronic applications. Semiconducting CNTs, for instance, seem to be

potential channel materials for transistors because their diameter may be controlled to customize optical and optoelectronic features. Carbon nanomaterials have often been suggested as a possible replacement to traditional semiconducting materials like silicon in electrical and optoelectronic applications for such reasons [1,2]. whereas metallic CNT thin films have been possibly useful as transparent conductors.

A CNT seems to be a three-terminal switch in which current flows via two electrodes

attached to the CNT [3,4]. Semiconducting CNTs have a straight band gap and exhibit both free electron-hole pair excitations and firmly bound electron-hole pair states known as excitons. [4] Because of the one-dimensional nature of CNT, van Hove singularities in the charge density occur, resulting in intense optical emission and absorption with energies defined by CNT chirality. Since strong Coulombic interactions, the exciton binding energies in CNT seem to be larger (few hundred meV) [5,6] than in traditional bulk semiconductors like GaAs (10 meV) [7,8]. Because one-dimensional excitons have a high binding energy, they have long radiation lifetimes (up to 100 ns) [9].

The fluorescence lifetimes (up to 100 ps) at ambient temp make studying exciton dynamics at room temp simple (while fabrication-intensive coupled-quantum well heterostructures of III-V semiconductors). [10,11]. Semiconducting CNTs seem to be viable candidates for electroluminescent and photocurrent apparatus in addition to photoluminescent applications. CNT has been used to make light-emitting transistors and photoelectronic devices. Since of their great charge movement of $10000 \text{ cm}^2/\text{Vs}$, long π -conjugation lengths, and broad aspect ratio ranging [12,13,14], CNTs have been employed as acceptors. Gallium Nitride (GaN) is indeed a direct bandgap binary III/V semiconductor, which is considered suitable for high-power transistors that can increase operational temps. It was widely employed in light emitting diodes since the 1990s (LED). Gallium nitride emits a blue light that is utilized to read Blu-ray discs. Gallium nitride is also found in semiconductor power apparatus, photonics, lasers, and radio frequency components. GaN will be used in sensor technologies in the future [15,16]. The bandgap of gallium nitride is 3.4 eV, while the bandgap of silicon is 1.12 eV. Because gallium nitride has a larger band gap than silicon MOSFETs, it can withstand greater voltages and temperatures. Gallium nitride has gained a lot of attention for applications including full-color or white light

emitting diode (LED) displays and backlighting for liquid crystal displays [17,18].

2- Experimental

2-1 Computational Method

The GaussView 5.0.8 application [19] has been utilised to create the complex's initial structure and supply the database for it. The computations were carried out with the help of the Gaussian 09 software package [20]. In the gas phase, B3LYP-SDD/DFT was used to completely relax CNT. All electronic structure estimates use the B3LYP mixture of exchange-correlation functional in DFT. The B3LYP/DFT technique using SDD basis sets was used to compute the electrical excited electrons for the relaxing metal cation. The B3LYP-SDD/DFT approach has been shown to be accurate in computing the spectra characteristics of the molecules under investigation.

2-2 Preparation of CNT

The CVD process involves the depositing of a strong on a warmed surface thru a vapour or gas phase concoction reaction [21]. A reaction between the vapour and similar substrate might frame the deposit. CNT coatings were applied on a glass surface. At different precipitation temperatures (300 to 900 degree centigrade) and nitrogen flow rates, CNT coatings treated with GaN were preserved. In this investigation, a gas-phase depositing process approach CVD (see Fig.1) has been used as another repeat for solid layer sedimentation. In this project, a gas-phase depositing process method has been used as a novel approach for hard layer formation. The powder dissipation equipment employed in this study consisted of a GSL-1600-60X high-temp vacuum tubes heater that supplied the gases for the sedimentation procedure [22]. The gas transmission system, which comprises of two feeding lines for CNT/Ga vapour and nitrogen gas, is utilized to provide all necessary gases into the chamber in a regulated manner. A flawless face layer was taken up at that time in the sedimentation chamber and that is the reactor for sedimenting CNT/GaN coatings. The exhaust gas device is then used to remove all non-responded chemical compounds, followed by the response manufacturing



Figure 1: Coating preparation tool utilized in the current investigation: 1. Part of Evaporation, 2. Path of Ti-Based vapor, 3. sedimentations Chamber, 4. Quartz pipe for sedimentations, 5. Exhausting gas part, 6. thermometer.

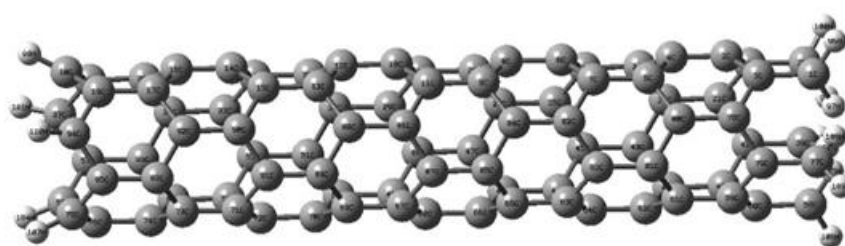
3- Results and Discussion

Using the combination functional B3LYP-DFT with SDD basis functions, the relaxing structure of CNT and CNT/GaN in Fig.2 has been

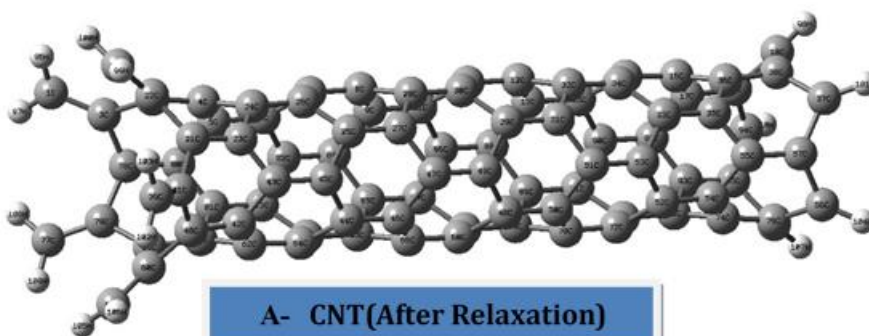
optimised at the minimum. Table 1 shows the determined magnitudes for the complex's optimum factors.

Table 1: The optimize factors for the CNT and CNT/GaN.

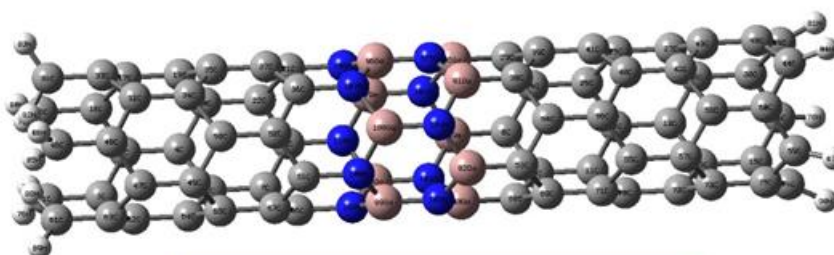
Bond	Value (nm)	
	CNT	CNT/GaN
C-C	0.1415	0.1424
C-H	0.1082	0.1098
C-N	-	0.1442
C-Ga	-	0.1485
N-Ga	-	0.1392



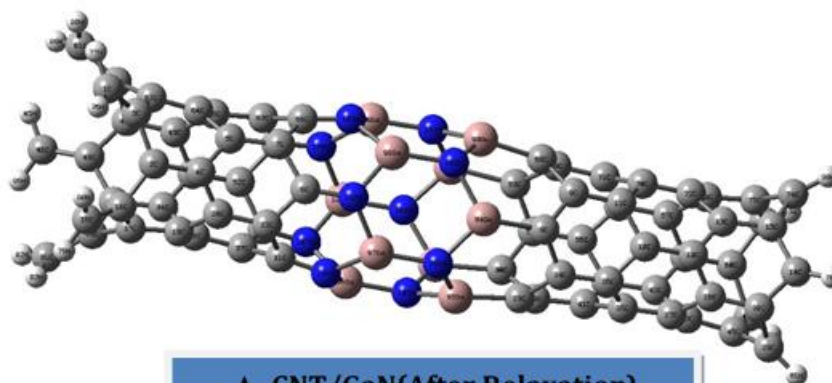
A-CNT(Before Relaxation)



A- CNT(After Relaxation)



A- CNT/GaN(Before Relaxation)



A- CNT/GaN(After Relaxation)

Figure 2: The optimized structures of CNT and CNT/GaN at B3LYP-DFT.

The results show that using a composite functional DFT-B3LYP with SDD basis functions to assess the improved structure of CNT seems to be useful. The improved structure of the CNT was discovered to be in good agreement with the experiment data. Table 2 shows the total energy ET in a.u and the virial proportion (-

V/T), as well as various estimated energies in eV for CNT and CNT/Ga, based on Koopman's theory. These simulations were conducted out using a B3LYP/6-31G level of DFT, with the electrode potential IE, electrons affinities EA, and Fermi energy X included. B3LYP-SDD/DFT-

based descriptors were derived to assess the

reactivity and stability of the complexes [23]:

$$\mu = \left(\frac{\partial E}{\partial N} \right)_{V(\vec{r}), T} \quad (1)$$

$$E_f = \frac{(IP + EA)}{2} \quad (2)$$

Table 2: Electronic calculations for CNT and CNT / GaN.

Sample	E _T	HOMO	LUMO	E _g	IP	EA	E _F
CNT	-2036.36588	-3.259	-3.202	0.056	3.259	3.203	-3.231
CNT/GaN	-2589.35479	-3.725	-3.632	0.093	3.726	3.633	-3.679

Note from the table (2), the results of the ground state total energy (ET) in (eV) of the CNT structures are listed in Table 2. The Pure CNT has the largest value of total energy, ET was decreased with increasing the number of Ga and N atoms. This findings reflects every structure's binding energy and demonstrates that these structures have excellent relaxation. This ensures that the impact of introducing N and Ga atoms to Pure CNT on the molecule's available power was effective [24,25].

The frontier atomic orbitals theory has been used to characterize the chemical characteristics of the examined system. The most significant molecular orbitals are HOMO and LUMO. The HOMO energy is a decent approximation to negative experimental ionization potential ($E_{\text{HOMO}} \cong -IP$) and the LUMO energy is equivalent to negative electron affinity ($E_{\text{LUMO}} \cong -EA$), according to the Koopmans' theorem. Therefore, the electronic characteristics of CNT in terms of LUMO and HOMO. The LUMO and HOMO energies are linked to the type of interactions between GaN and CNT atoms. The interaction of border atomic orbitals seems to be responsible for the onset of the interaction of two reactants in quantum mechanics [26,27]. The notion of HOMO and LUMO energies may also be used to describe the categorization of interactions between CNTs and GaN atoms. HOMO may donate electrons, whereas LUMO can deduct electrons. Nevertheless, if a molecule absorbs a large amount of HOMO energy, it will become more unstable due to increased reactivity, and

vice versa. For CNT/GaN, the HOMO and LUMO orbitals have energies of -3.725 eV and -3.632 eV, respectively.

The findings demonstrated that the forbidden energy gap E_g of all structures are few, and thus the investigated CNT have high conductivity and small forbidden energy gap. Pure CNT has (0.056 eV), adding more Ga and N atoms in place of carbon C in the Pure CNT leads to increase the forbidden energy gap of the structure. The reasons of this result are due to the constructed molecular orbitals MOs from the linear combination of atomic orbitals LCAOs, in which the atoms G, N and C have different values of electronegativity [28,29,30].

Table 2 demonstrates the calculated magnitudes of the ionization potential IP and electron affinity EA of the structures under study, where the IP and EA are increased with Adding the Ga and N atoms to the CNT. The IP was increased from (3.259 eV) for Pure CNT to (3.726 eV) for CNT/GaN. Also, the EA was increased with increasing the Ga and N atoms in the CNT. These results indicate that the doped CNT has a high ability to donating or accepting an electron to become a cation or anion [20,31].

The results in Table 2 showed that the Fermi energy values increase with add of Ga and N atoms added in place of C. The Fermi energies of Pure CNT and CNT/GaN seem to be large in general, indicating that the electron in such structures have such a high escape propensity and a reduction in the HOMO and LUMO energies [18,32,33,].

Density of states (DOS) analysis

The DOS is responsible for a variety of physical characteristics and thus plays a significant function in condensed matter physics. The ability to forecast how the DOS would behave for various nanostructure geometries is critical. The DOS of a system refers to the number of states, which were accessible to be inhabited per period of energy at every level of energy. The number of possible states in a particular energy interval affects the distribution of energy amongst identical particles [5].

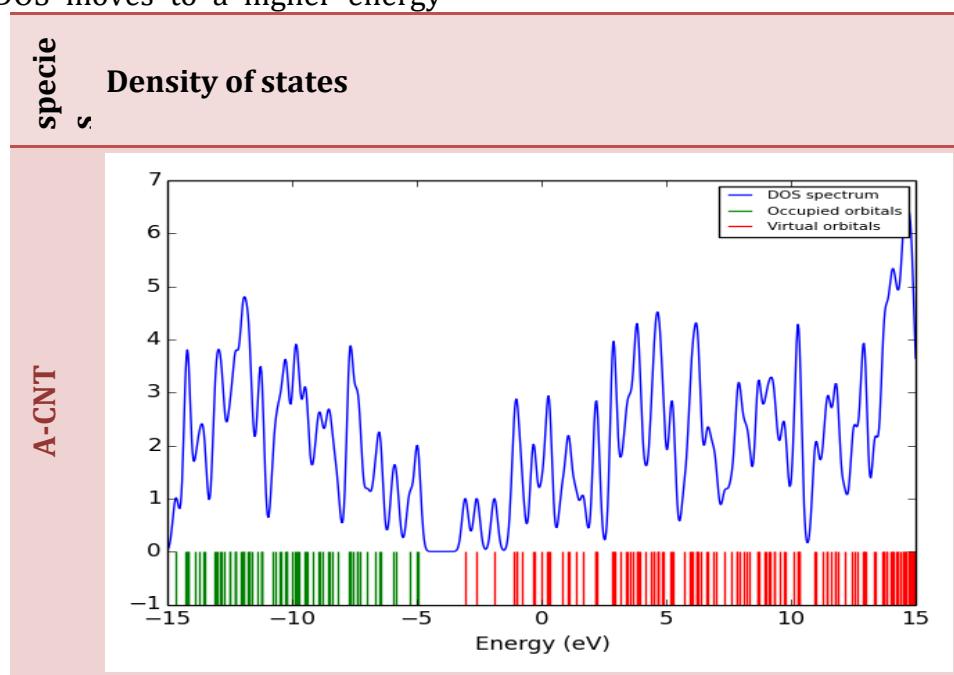
Figure 1 shows the DOS of Pure CNT as a functions of Fermi energy determined using the LDA/SZ DFT (3). The nonzero DOS suggests that there are a limited number of states. In the accessible of local possible oscillations in the CNT, this is most probable. A typical frequency of the oscillations of 3.5 eV may be estimated from the DOS distribution. Figure (3) showed that the pure CNT has more solubility than the CNT/GaN, this is depending on the linear combination of atomic orbitals to form molecular orbitals due to presence the Ga and N atoms resulting from the participation of all atoms C, N and Ga, while pure CNT orbits are the result of only carbon (C) atoms [34,35]. Nevertheless, the electrical property of CNT is impacted by the interactions with GaN atoms, in which the DOS moves to a higher energy

area and also a notable DOS peak occurs just above Fermi level for most configurations, indicating variance in conductivity. As illustrated in the illustration (3).

As can be observed in all CNT/GaN systems, their DOS around the LUMO level varies significantly from that of CNT, leading in a decrease in the band gap and, as a consequence, an increase in electrical conductivity. The difference in energy between the HOMO (valent level) and the LUMO (heat transfer level) for insulator and semiconductors is referred to as the band gap in DOS plots. This is the energy required to liberate an outer shell electrons from its orbital and transform it into a mobile charge transfer that can freely transfer throughout the material. As illustrated in [25, 28], the conduction band seems to be an important component in influencing a material's electrical properties:

$$\sigma \propto \exp\left(-\frac{E_g}{2k_B T}\right) \quad (3)$$

where T and σ , k_B , were the conductivity, the temp 298.14 K, and the Boltzmann's constants, respectively. Depending on this formula, smaller magnitudes of band gap at a assumed tem caused greater electrical conductivity.



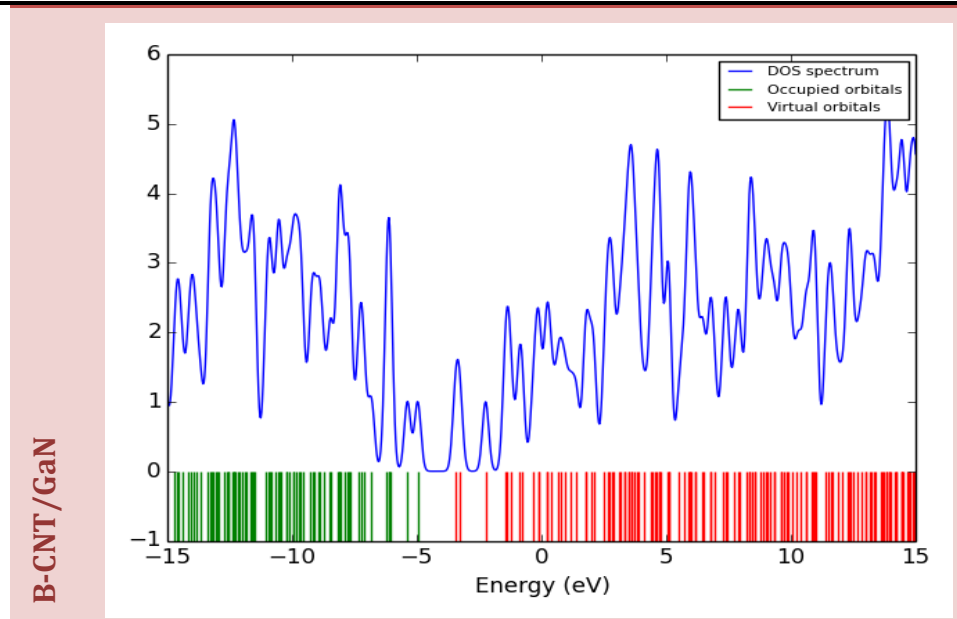


Figure 3. The DOS the CNTs in this work .

Scanning Electron Microscope of CNT/GaN

The morphology of the CNT/GaN synthesized at 300 °C and (B) 900 °C on a glass substrate with different magnification were investigated by scan electrons microscopes (SEM) and shown in figure 4 (A and B) While the SEM images showed the correctness of the carbon tube preparation and the success of the grafting process.

Fig.4-A shows the SEM pictures of the CNT coatings on the extremely high surface area unit. The surface has been characterised by amorphous structures with numerous globose tiny droplets, which have been created during the condensing of the gas phase, according to

the low temp deposition specimens (at 300 degree centigrade). In the case of CNT coatings, increasing the deposition temp to 900 degree centigrade (see Fig.4) might result in morphological changes in the form of a thick and intense extra crystal structures. A thick coating of boron nitride composite GaN nanowires with similar diameter is seen in fig.4-B at 900 degree centigrade. The BN nanowires have been made without the usage of catalytic particles, depending on our approach. Since no large particles have been identified at the ends of nanowires, the terminals had the same size as the nanowire body [36,37]

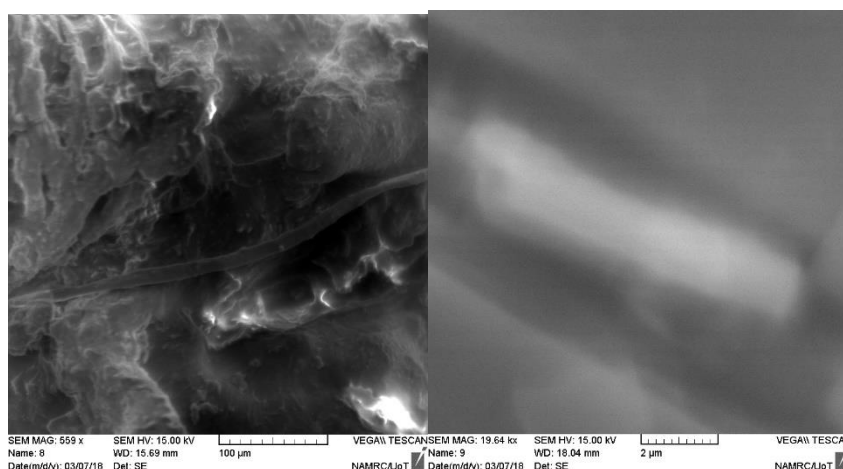


Fig.4-A SEM of CNT layer placed at (A)300 °C and (B) 900 °C on glass substrate with various magnification.

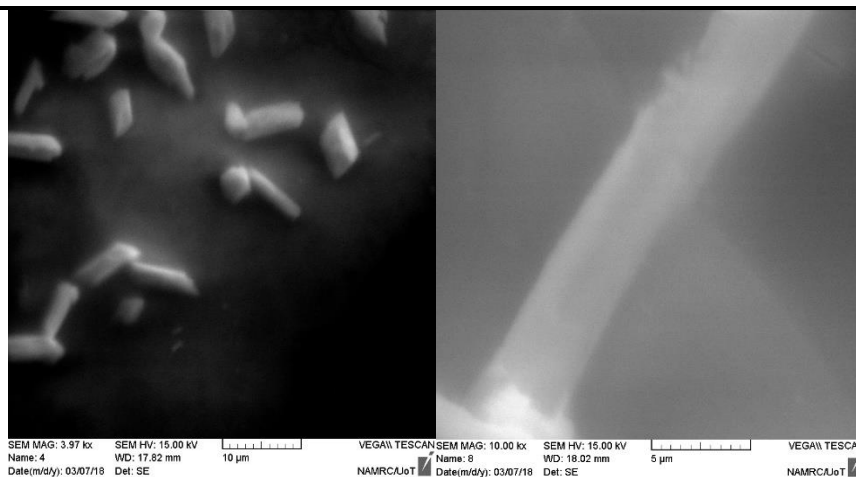


Fig.4-B SEM of CNT/GaN layer placed at (A)300 °C and (B) 900 °C on glass substrate with different magnification

4- Conclusions

The activity of several proposed Titanium Metal Complexes was investigated using B3LYP-SDD/DFT predictions based on the coordinating of these complexes. The findings revealed that the Ti bonds were consistent with those found in experimental observations. The complex's activity was predicted using softness, global hardness, energy gap, and frontier orbitals (ELUMO and EHOMO). The quantum chemistry characteristics revealed that the Titanium Tetrafluoride metals combination had a small energy gap and a high activity for interacting with other species. Coating has been seen to be continuous and uniform. Titanium has been produced as a globular film during the whole surface. Many holes may be visible at higher magnifications (50,100,200 nm), and grain sizes were observed to be smaller (10-20 nm).

References

1. Zhang, H., Yan, S., Wang, T., Wu, Y., Zhao, X., & Zhao, N. (2020). Enhanced heat transfer of carbon nanotube nanofluid microchannels applied on cooling gallium arsenide cell. *Journal of Thermal Science*, 29(6), 1475-1486.
2. Melisi, D., Nitti, M. A., Valentini, M., Valentini, A., Ligonzo, T., De Pascali, G., & Ambrico, M. (2014). Photodetectors based on carbon nanotubes deposited by using a spray technique on semi-insulating gallium arsenide. *Beilstein journal of nanotechnology*, 5(1), 1999-2006.
3. Cholewa, M., Moser, H. O., Huang, L., Lau, S. P., Yoo, J., An, S. J., ... & Fischer, B. (2007). Secondary electron emission properties of III-nitride/ZnO coaxial heterostructures under ion and X-ray bombardment. *Nuclear Instruments and Methods in Physics Research Section B: Beam Interactions with Materials and Atoms*, 254(1), 55-58.
4. Habeeb SA, Hasan AS, Țălu Ș, Jawad AJ. Enhancing the Properties of Styrene-Butadiene Rubber by Adding Borax Particles of Different Sizes. *Iran. J. Chem. Chem. Eng. Research Article Vol.* 2021;40(5): 1616-1629.
5. Y. Ellahioui, S. Prashar, and S. Gómez-Ruiz, "Anticancer applications and recent investigations of metallodrugs based on gallium, tin and titanium," *Inorganics*. 2017.
6. Hasan AS, Mohammed FQ, Takz MM. Design and Synthesis of Graphene Oxide-Based Glass Substrate and Its Antimicrobial Activity Against MDR Bacterial Pathogens. *Journal of Mechanical Engineering Research and Developments*. 2020.
7. Jin, Y., Li, Q., Li, G., Chen, M., Liu, J., Zou, Y., ... & Fan, S. (2014). Enhanced optical output power of blue light-emitting diodes with quasi-aligned gold nanoparticles. *Nanoscale Research Letters*, 9(1), 1-6.
8. Thamer AD, Hasan AS, Kadhim RG, Bakheet WG, Abbood HI. Carbon Nanotubes Sensors for Gases Detection

- in Oil Industry. *Journal of Petroleum Research and Studies*. 2018;8(3):25-40.
9. Olegovich Bokov, D., Jalil, A. T., Alsultany, F. H., Mahmoud, M. Z., Suksatan, W., Chupradit, S., ... & Delir Kheirollahi Nezhad, P. (2022). Ir-decorated gallium nitride nanotubes as a chemical sensor for recognition of mesalamine drug: a DFT study. *Molecular Simulation*, 1-10.
 10. Ati AA, Abdalsalam AH, Hasan AS. Thermal, microstructural and magnetic properties of manganese substitution cobalt ferrite prepared via co-precipitation method. *Journal of Materials Science: Materials in Electronics*. 2021 Feb;32(3):3019-37.
 11. L. Kong et al., "Phase I/II trial evaluating concurrent carbon-ion radiotherapy plus chemotherapy for salvage treatment of locally recurrent nasopharyngeal carcinoma," *Chin. J. Cancer*, 2016.
 12. Abud SH, Hasan AS, Almaamori M, Bayan N. Enhancement the ability to pump crude oil using rubber solutions. In *Journal of Physics: Conference Series* 2021 Mar 1 (Vol. 1818, No. 1, p. 012235). IOP Publishing.
 13. Chen, C. C., Yeh, C. C., Chen, C. H., Yu, M. Y., Liu, H. L., Wu, J. J., ... & Chen, Y. F. (2001). Catalytic growth and characterization of gallium nitride nanowires. *Journal of the American Chemical Society*, 123(12), 2791-2798.
 14. R. M. German, "Progress in titanium metal powder injection molding," *Materials (Basel)*, vol. 6, no. 8, pp. 3641-3662, 2013.
 15. Jacobs, B. W., Ayres, V. M., Crimp, M. A., Ronningen, R. M., Zeller, A. F., Shaw, H. C., ... & Petkov, M. P. (2004). Investigation of Resiliency of Carbon Nanotubes and Gallium Nitride Nanocircuits to Simulated Space Radiation. *MRS Online Proceedings Library (OPL)*, 851.
 16. S. Lacombe, E. Porcel, and E. Scifoni, "Particle therapy and nanomedicine: state of art and research perspectives," *Cancer Nanotechnology*. 2017.
 17. Hashim, D. P. (2014). Carbon Nanotube Doping Procedures for Three-Dimensional Macro-Structures and Gallium-Nitride Functionalization (Doctoral dissertation, Rice University).
 18. N. Usami, Y. Furusawa, K. Kobayashi, H. Frohlich, S. Lacombe, and C. Le Sech, "Fast He²⁺ ion irradiation of DNA loaded with platinum-containing molecules," *Int. J. Radiat. Biol.*, 2005.
 19. R. Dennington, K. Todd and M. John, "GaussView 5.0. 8.," Gaussian Inc 340, 2008.
 20. M. J. Frisch et al., "Gaussian09 Revision D.01, Gaussian Inc. Wallingford CT," Gaussian 09 Revision C.01. 2010.
 21. Kadem BY, Al-Hashimi M, Hasan AS, Kadhim RG, Rahaq Y, Hassan AK. The effects of the PEDOT: PSS acidity on the performance and stability of P3HT: PCBM-based OSCs. *Journal of Materials Science: Materials in Electronics*. 2018 Nov;29(22):19287-95.
 22. Thamer AD, Mohammed FQ, Hasan AS, Abid AL. Corrosion resistance enhancement in acidic solution for austenitic stainless steel by gas-phase hybrid deposition process. *Engineering and Technology Journal*. 2017 Oct 28;35(8 Part A):788-94.
 23. Abed AL. Synthesis and Study of Modified Nanostructure Porous Silicon Layers for Chemical Gas Sensing. *Engineering and Technology Journal*. 2017;35(10 Part A).
 24. Hasan AS, Abbood HI. Density Function Theory Calculations of Graphene Sheet. *Al-Kufa Journal of Physics*. 2016 Jun 10;9:59-65.
 25. Gokhale, V. J., Sui, Y., & Rais-Zadeh, M. (2012, May). Novel uncooled detector based on gallium nitride micromechanical resonators. In *Infrared technology and applications XXXVIII* (Vol. 8353, pp. 442-447). SPIE.
 26. Jebur SK, Braihi AJ, Hassan AS. Graphene effects on the structural, morphological

- and optical properties of PEDOT: PSS thin films. *Materials Today: Proceedings*. 2021 Oct 12:49(7): 2733-2740.
27. Hu, J., Bando, Y., Golberg, D., & Liu, Q. (2003). Gallium nitride nanotubes by the conversion of gallium oxide nanotubes. *Angewandte Chemie*, 115(30), 3617-3621.
28. Hasan AS, Akraa MA, Abbas SJ. Theoretical and Experimental Study for New Titanium Metal Complexes in Biophysical Applications. *Journal of Southwest Jiaotong University*. 2019;54(6).
29. Shokri, A., & Averagesi, F. G. (2013). First principal study on optical properties of carbon and gallium nitride nanotubes. *Optics Communications*, 304, 143-147.
30. Mohammed FQ, Edan MS, Hasan AS, Haider AJ. Synthesis and Theoretical Concepts of Boron Nitride Nanowires Grown on Nitrides Stainless Steel Surface by Hybrid Gas Phase Process. *In Key Engineering Materials 2021 (Vol. 886, pp. 97-107)*. Trans Tech Publications Ltd.
31. Khan, M. A. H., & Rao, M. V. (2020). Gallium nitride (GaN) nanostructures and their gas sensing properties: a review. *Sensors*, 20(14), 3889.
32. Hasan AS, Kadem BY, Akraa MA, Hassan AK. PVA: PEDOT: PSS: carbon based nano-composites for pressure sensor applications. *Digest Journal of Nanomaterials and Biostructures*. 2020 Jan 1;15(1):197-205.
33. Bachilo, S. M., Strano, M. S., Kittrell, C., Hauge, R. H., Smalley, R. E., & Weisman, R. B. (2002). Structure-assigned optical spectra of single-walled carbon nanotubes. *science*, 298(5602), 2361-2366.
34. Kadhim MH, Hasan AS, Akraa MA, Layla AY. Preparation and optimization of heterojunction donor (DLC)-acceptor (SI) as a solar cell by DFT and PLD. *Journal of Ovonic Research* Vol. 2021 May;17(3):273-81.
35. Xiong, Y., Cui, X., Zhang, M., Wang, Y., Lou, Z., & Shan, W. (2020). Microwave hydrothermal synthesis of gallotannin/carbon nanotube composites for the recovery of gallium ion. *Applied Surface Science*, 510, 145414.
36. Akraa M, Hasan AS, Kadhim MJ. Spectroscopy Characterization of Ethylene Vinyl Acetate Degradation by Different Kinds of Accelerated Aging. *Baghdad Science Journal*. 2020 Jul 12;17(3):0795-.
37. Jafari, S. N., Ghadimi, A., & Rouhi, S. (2019). Improving the efficiency of GaAs solar cells using a double semi-transparent carbon nanotubes thin layer. *The European Physical Journal Applied Physics*, 88(2), 20401.